Matematisk-fysiske Meddelelser
udgivet af
Det Kongelige Danske Videnskabernes Selskab
Bind **32**, nr. 14

Mat. Fys. Medd. Dan. Vid. Selsk. **32**, no. 14 (1960)

OPTICAL HYPERFINE STRUCTURE OF NEON-21

BY

EBBE RASMUSSEN(†) AND V. MIDDELBOE

København 1960
i kommission hos Ejnar Munksgaard

Printed in Denmark
Bianco Lunos Bogtrykkeri A-S

Introduction

The hyperfine structure in the spectrum of Neon-21 was investigated for the first time by KOCH & RASMUSSEN[1] more than ten years ago. In this investigation some of the hfs components of Ne^{21} were masked by partially unseparated Ne^{20}. Nevertheless, it was still possible to obtain the following results: the nuclear spin of Ne^{21} is $^3/_2$ (possibly greater) and the nuclear magnetic moment is negative. In recent years, both these observations have been confirmed by the use of modern experimental methods; thus, HUBBS & GROSOF[2] have established with certainty that $I = {}^3/_2$, and RAMSAY et al.[3] have determined the value of $\mu = -0.66176$ n.m.

In 1955, K. CLUSIUS, Zürich, kindly has sent one of us (E.R.) a very highly enriched Ne^{21} sample (about 1 c.c. at atm. pressure). The spectroscopical investigation of the hfs of Ne^{21} was resumed soon after the receipt of this generous gift in which the Ne^{21} concentration had been enriched (from 0.3 % in natural Neon) to very nearly 99 % pure by repeated thermal diffusion. The renewed optical investigation led to a determination of the hfs splitting in a number of terms of the Ne^{21} arc spectrum. In the case of the $2s_5$ term (Paschen notation), a precise determination of the hfs splitting has recently been obtained by RABI et al.[4] working with an atomic beam resonance method.

In many respects our spectroscopical procedure was much the same as that previously used, and it is given in detail, for example, in the description of some investigations on separated Krypton isotopes[5]. However, certain experimental modifications were necessary, partly because the Neon was provided in the gaseous state (Kr had been collected in Aluminium), and partly because of the large Doppler width of the spectral lines (twice that of Kr) in combination with the rather narrow splittings (one third those of Kr) — line broadening had now in fact become the limiting experimental factor.

Experimental Modifications

Using the apparatus sketched in Fig. 1, the Ne^{21} gas was transferred to a number of "seeds", i.e., closed glass tubes about 0.5×1 mm in diameter and a few centimetres long. Furthermore, the discharge tube was given

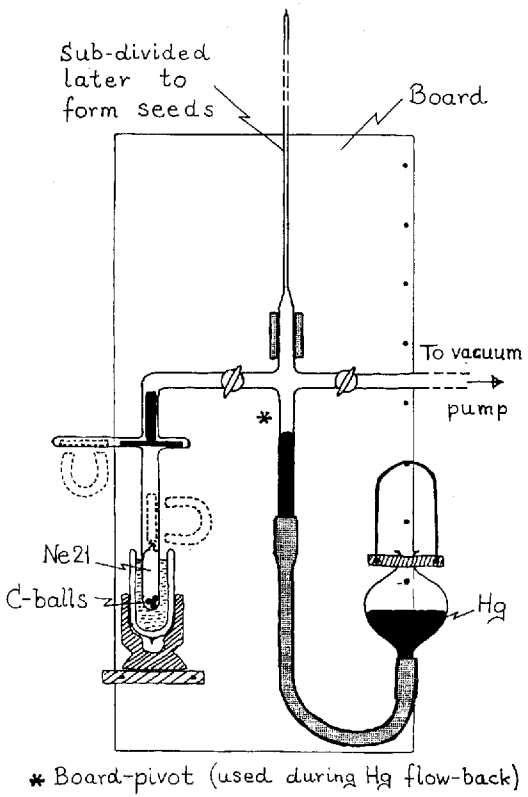

Fig. 1. Neon-21 transfer apparatus. Scale: approximately 1/10.

the modified shape shown in Fig. 2. Hereby it was possible to make use of a technique, developed many years ago[6], which consists in breaking open one or more seeds inside the sealed-off discharge tube.

Helium from Canada (free from Ne) was used as a carrier gas, and in order to reduce the broadening of the Ne^{21} lines, the Helium pressure was kept lower than usual (2—3 mm Hg instead of 10), although this inevitably shortens the life of a discharge tube. The pressure of Ne^{21} was estimated

at 0.1 mm Hg for each seed that was liberated. Up to three or four seeds were liberated consecutively during the life span of each discharge tube.

In an attempt to reduce the temperature of the liquid air used for cooling the discharge, the Dewar containing the cooling medium was closed with a large rubber stopper (penetrated by the U-shaped part of the discharge tube) and, during exposure, the pressure above the cooling medium was kept down at 15—20 mm Hg by means of continuous mechanical pumping via a $^1/_2$ inch exhaust pipe. On starting the pump, the liquid air would bubble violently for a short time, no doubt while its nitrogen content was boiling off,

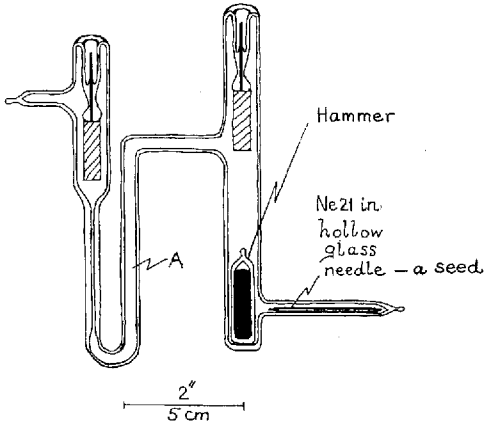

Fig. 2. Discharge tube.

but soon the remaining liquid (oxygen) became perfectly calm—presumably at a temperature of 60—65° K. A $^3/_4$ inch steel ball resting on the top of a $^1/_2$ inch bore through the rubber stopper constituted a combined refilling device and safety valve.

The Joule heat evolved in the He-Ne-gas was kept as low as possible by reduction of the discharge current to a minimum (1—2 mA). Furthermore, the discharge in the thin-walled part of the tube, "A" in Fig. 2, was spectographed instead of that in the capillary part of the tube normally used. These modifications, in connection with the lowered temperature of the cooling medium, reduced the Doppler width sufficiently (20—40 %) and made it just possible to resolve a number of the hfs components. This was only achieved, however, at the cost of a considerable loss in luminance.

The unavoidable reduction in the brightness of the discharge was compensated by a five- to ten-fold increase in the transmission of the Fabry-Perot interferometer. This was achieved by coating each quartz plate with

seven alternate layers of zinc sulphide and cryolite—instead of the silver layer normally used. Moreover, the resolving power of these multilayers was perfectly adequate in the whole of the spectral region (yellow-orange) that was investigated.

Finally, a new étalon spacer of optimum thickness (40 mm) was produced with a tolerance far better than 1 mil.

Measurement of Line Structure Intervals

The spectroscopically resolved hyperfine structure (hfs) of seven Ne^{21} spectral lines was measured. All the measured lines represent $1s-2p$ combinations, and their wavelengths are given in Table 1. Each measurable interval in the structure of these seven lines was determined 5—15 times, using the best out of 83 exposures.

TABLE 1.

Wavelength Å.	Transition
5852	$1s_2-2p_1$
5881	$1s_5-2p_2$
6030	$1s_4-2p_2$
6074	$1s_4-2p_3$
6266	$1s_3-2p_5$
6598	$1s_2-2p_3$
6717	$1s_2-2p_5$

A plate showing three of the investigated spectral lines is reproduced on page 7.

The mean values of all the measured line intervals are collected in Table 2, and given there in units of 10^{-3} cm^{-1}. These values are believed to be correct to within 1—2 units. The sequence of the intervals given in the last column of Table 2 is in accordance with the *increasing* energy of the hfs components; in an interferogram (Plate 1, page 7), this corresponds to moving through a single order *away from* the centre of the photographic plate. In Table 2, the J-value of each term is noted directly below the term symbol in question.

At the bottom of Figs. 3—7, the hfs patterns of five of the measured spectral lines are shown. The height of each line pattern component is drawn

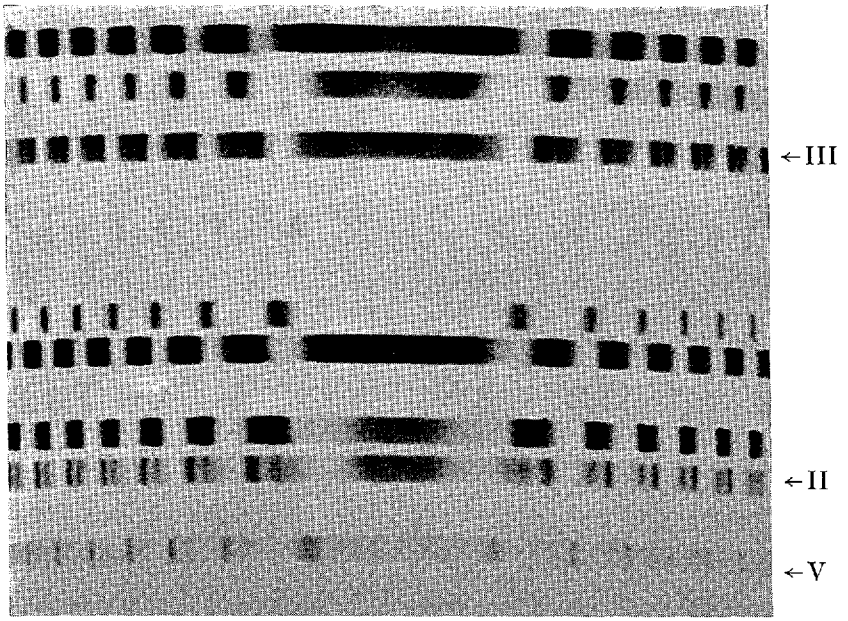

Plate 1. An interferogram of Neon-21. V: 6030 Å. II: 6074 Å III: 6266 Å. 6—7 orders are to be seen on each side.

TABLE 2.

Ne^{21} spectrum	Lower term	Upper term	Total line splitting $\times 10^{-3}$ cm^{-1}	Measured intervals $\times 10^{-3}$ cm^{-1}
Line I.....	$1s_2$	$2p_1$	82	25 57
	$J=1$	0		
„ II.....	$1s_4$	$2p_3$	66	27 39
	$J=1$	0		
„ III.....	$1s_3$	$2p_5$	62	37 25
	0	$J=1$		
„ IV	$1s_2$	$2p_2$	88	27 61
	$J=1$	1		
„ V	$1s_4$	$2p_2$	71	29 42
	$J=1$	1		
„ VI	$1s_5$	$2p_2$	76	12 24 40
	$J=2$	1		
„ VII	$1s_2$	$2p_5$	89	54 35
	$J=1$	$J=1$		

proportional to its calculated intensity, and the mean value of each interval that could be measured is given below the corresponding line pattern. ν stands for the wave number which, of course, is proporional to the energy.

Determination of Term Component Separations

In the case of the spectral lines I, II, and III (Table 2), the line splittings are directly equal to the splittings of the terms $1s_2$, $1s_4$, and $2p_5$, respectively, because in each case the combining term has $J = 0$. In Figs. 3 and 4, the respective term diagrams of the two lines, I (5852 Å) and III (6266 Å), are

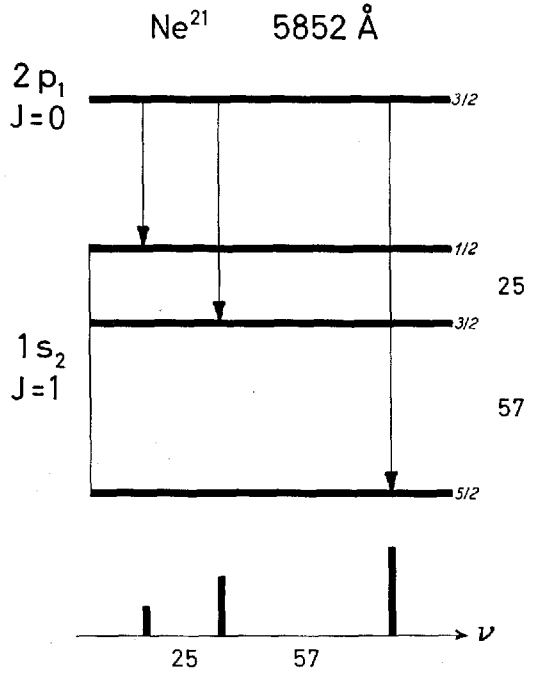

Fig. 3. Spectral line I.

given above the line patterns. In each term diagram the F-values are given directly to the right of the term components, and the separations are noted —also to the right—in between the hfs term components in question.

The term component separations that have been determined are noted in the third column of Table 3 (in units of $10^{-3}\,\mathrm{cm}^{-1}$). A separation is given there as positive, when the upper (i.e. more energetic) hfs component has the higher F-value.

In Table 2 a comparison between the lines I and IV on the one hand, and II and V on the other, shows immediately that the splitting of the term $2p_2$ is rather small. The separations between the $2p_2$ components can be estimated, for example, from the measured intervals of line V (6030 Å), by the following "trial and error" procedure (see Fig. 5). Assume the separations between the $1s_4$ components (already found from line II) to be correct, assign arbitrary separations to $2p_2$, construct the line structure pattern (bottom of Fig. 5) and determine the "centres of gravity" of the resulting groups of line components. The selected assignment of the $2p_2$ separations is that which results in intervals between the aforementioned centres of

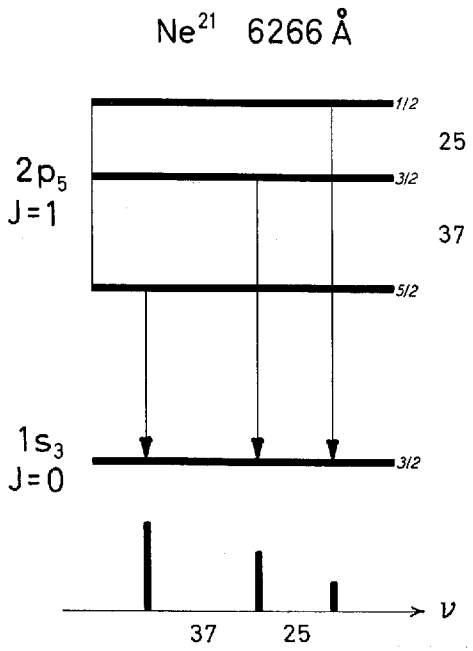

Fig. 4. Spectral line III, which can be compared with III in Plate 1.

gravity (dotted lines in fig. 5), that turn out to be equal to the observed values, viz., 29 and 42 units.

Using the trial and error method just described, the hfs separations of $2p_2$ were evaluated at 6 and 4 units, respectively. The relative uncertainty of the ratio of these two separations, i.e. 6:4, is naturally rather great, but the uncertainty of the total splitting, 10 units, is fair — maybe 20 %. The result is included in Table 3. The opposite sign of the splitting of this term

as compared with the other terms is analogous to what has previously been found for isotopes of other noble gases[5)7)].

Adopting the estimated values for the $2p_2$ separations and applying the trial and error method described above, the separations of the term

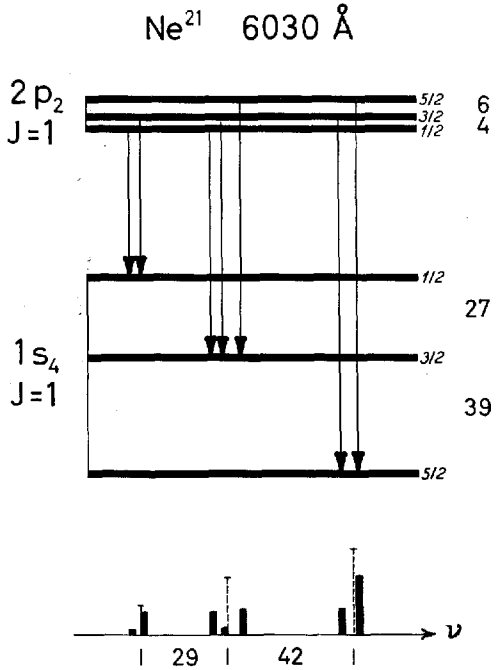

Fig. 5. Spectral line V.

$1s_5$ have been found from the measured intervals of line VI (5881 Å). The result is shown in Fig. 6, and given in Table 3 along with the observed separations of the other four terms.

Finally, line VII (6717 Å) gives a check on the hfs separations of the

TABLE 3.

Term	J-value	Separations			Total
$1s_2$	1	−57	−25		−82
$1s_4$	1	−39	−27		−66
$2p_5$	1	−37	−25		−62
$2p_2$	1	(+6)	(+4)		+10
$1s_5$	2	−36	−20	−10	−66

terms $1s_2$ and $2p_5$. The measured splittings of these two terms, as determined from lines I and III, lead to the structure pattern of line VII shown at the bottom of Fig. 7. The resolution obtained spectroscopically permitted the measurement of the two intervals that are bounded by the two dotted lines

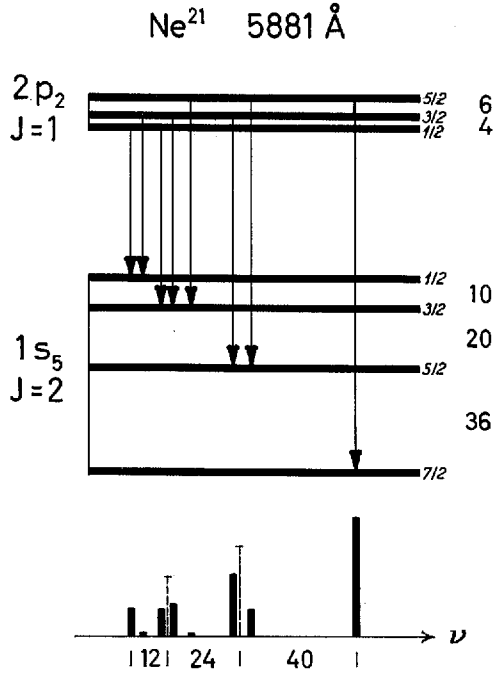

Fig. 6. Spectral line VI.

and the most energetic line component. By *calculation* from the previously determined splittings of $1s_2$ and $2p_5$ the magnitude of these two intervals is found to be equal to 52.5 and 35.5 units (total: 88 units). The corresponding directly *observed* values, as noted in Table 2, are 54 and 35 units (total: 89 units), which constitutes a satisfactory agreement.

Theoretical Discussion

Assuming the following formula to be valid for the energy of an hfs term component

$$E = E_0 + a\frac{C}{2} + b\left[\frac{\frac{3}{4}C(C+1) - I(I+1)J(J+1)}{2I(2I-1)J(2J-1)}\right],$$

where $C = F(F+1) - I(I+1) - J(J+1)$, and using the value $I = {}^3/_2$, the interval factors (interaction constants) a and b in Table 4 have been computed (evaluated) from the hfs sparations given in Table 3. The a- and b-values in Table 4 should be experimentally correct to within 0.5—1 unit of 10^{-3} cm^{-1}.

The graphically evaluated a and b constant for the term $1s_5$ (see Fig. 8)

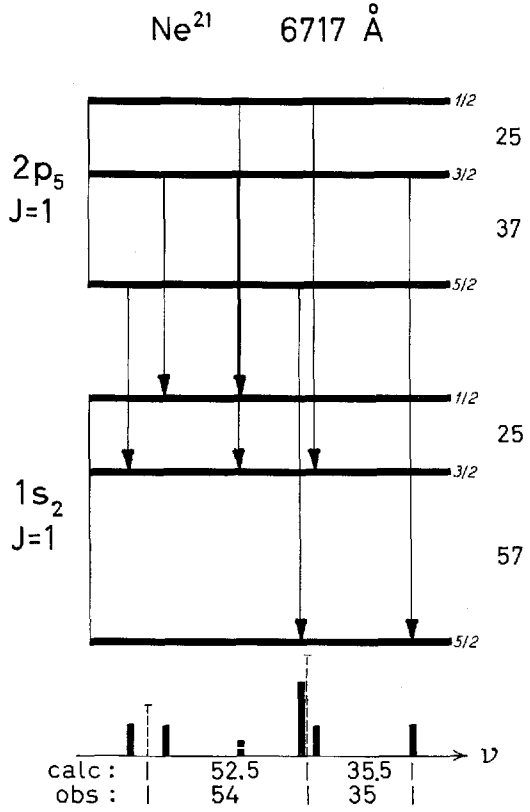

Fig. 7. Spectral line VII.

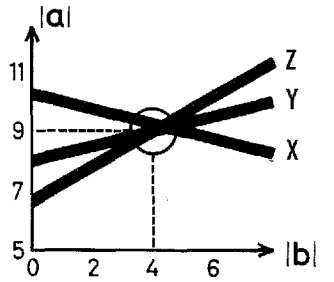

Fig. 8. Graphical evaluation of a and b from the following observed hfs separations of $1s_5$: 36 units (X), 20 units (Y), and 10 units (Z). The width of the graphical lines (X, Y, and Z) indicates the extent of the estimated experimental error.

may be used to re-calculate a set of mathematically consistent values for the hfs separations of this term. This procedure yields the separations 35, 20, and 10 in the optical units, or in Mc/sec: 1050, 600, and 300, which compares well with the high-precision values 1034.48, 599.44, and 303.93, measured by Grosof, Buck, Lichten, and Rabi. These latter values correspond to $a(1s_5) = -8.93$ and $b(1s_5) = -3.72$ in units of 10^{-3} cm^{-1}.

An analysis of the hfs separations may be performed in analogy to that of the Xe-[7] and Kr-spectra[5]. The most reliable determination of the nuclear quadrupole moment is obtained from the interval factors of the $1s_5$ term, which may be regarded as a rather pure configuration consisting of a $3s$ electron plus the ion in a $^2P_{3/2}$ state, corresponding to a "hole" of the $p_{3/2}$ type. Only the hole contributes to the quadrupole coupling. The determination of Q involves an estimate of $\overline{r^{-3}}$ for the hole (cf., e.g., expressions (7) and (8) in ref. [7]), and this can be obtained either from the fine structure separation Δ of the ion (cf., e.g., expression (9) in ref. [7]) or from the magnetic coupling between the hole and the nucleus. The latter procedure, employed in ref. [4], involves as a first step an estimate of the magnetic

TABLE 4.

Term	a	b
$1s_2$	−21	−3
$1s_4$	−16	+1
$1s_5$	− 9	−4
$2p_2$	+2.5	(0)
$2p_5$	−15	+1

coupling of the s-electron, which, from the Fermi-Segré formula, is found to be $a(s) = -8.1$. Now, since $a(1s_5) = \frac{1}{4}\, a(s) + \frac{3}{4}\, a(P_{3/2})$, one finds $a(P_{3/2}) = -9.2$ as the interval factor value for the ion. This in turn leads to $\overline{a_0{}^3 r^{-3}} = 12.4$ (cf., e.g., equation 13 in ref. [7]). Using this value, GROSOF et al.[4] found $Q = +0.093$, with an estimated error of 10 % due to the uncertainty in $\overline{r^{-3}}$. Moreover, the Sternheimer correction arising from polarization effects has been neglected. On the basis of the empirical fine structure separation ($\Delta = 782\ \mathrm{cm}^{-1}$) one obtains the alternative estimate $\overline{a_0{}^3 r^{-3}} = 11.2$, if one assumes an effective nuclear charge of $Z_i = Z - 2 = 8$. Within the estimated uncertainty the two values for $\overline{r^{-3}}$ are consistent.

For the terms $1s_2$ and $1s_4$, the wave functions can be written in the form

$$\psi = c_1 \varphi(\tfrac{3}{2}, \tfrac{1}{2}) + c_2 \varphi(\tfrac{1}{2}, \tfrac{1}{2}),$$

which represents a superposition of states with the hole in the $p_{3/2}$ and $p_{1/2}$ levels, while the outer electron is in the $3s$ level. The coefficients c_1 and c_2 can be computed from the atomic g-factors as well as from the multiplet separations; these two determinations agree well and both give for the $1s_4$

term the alternative possibilities ($c_1 = 0.77$, $c_2 = 0.64$) or ($c_1 = 0.34$, $c_2 = 0.94$).

By means of the above-mentioned wave functions one can calculate the a- and b-factors for the terms $1s_2$ and $1s_4$ on the basis of those belonging to the $1s_5$ term, if one applies expressions given by CASIMIR[8] (cf. also ref. [7]). We first note that the sum of the interval factors for $1s_2$ and $1s_4$ is independent of c_1 and c_2, and given by

$$a(1s_2) + a(1s_4) = \tfrac{1}{4}\, a(s) + \tfrac{5}{4}\, a(P_{3/2}) + \tfrac{1}{2}\, a(P_{1/2})$$
$$b(1s_2) + b(1s_4) = \tfrac{1}{2}\, b(P_{3/2}) = \tfrac{1}{2}\, b(1s_5),$$

where $a(P_{1/2})$ is the interval factor for the $p_{1/2}$ hole. Assuming $a(P_{1/2}) = 5\, a(P_{3/2})$, holding for a non-relativistic p-electron, and using the above quoted values for $a(s)$ and $a(P_{3/2})$, one finds $a(1s_2) + a(1s_4) = -37$, which agrees well with the values in Table 4. Also the sum rule for the b-factors is seen to be fulfilled.

In the non-relativistic case, the individual b-factors involve the same combination of c_1 and c_2 as the g-factors, and for $1s_2$ and $1s_4$ one then has the following relation:

$$b = -3\,(g-4)\; b(1s_5).$$

Using $g(1s_2) = 1.034$ and $g(1s_4) = 1.464$, and $b(1s_5) = -3.7$, one obtains $b(1s_2) = -3.3$ and $b(1s_4) = +1.4$ in good agreement with the optically determined values.

The a-factors differ in accordance with the alternative sets of c-coefficients; both these c-sets (quoted above) can be derived from the Zeeman effect and from the multiplet separation. The first c-set gives $a(1s_2) = -22$ and $a(1s_4) = -15$, while the second c-set gives $a(1s_2) = -13$ and $a(1s_4) = -24$. Thus, the magnetic hfs splitting (Table 4, column a) provides strong evidence in favour of the first set ($c_1 = 0.77$, $c_2 = 0.64$).

The p-terms have a more complex structure since, for the terms considered, neither the ion nor the outer electron has a definite j.

Acknowledgements

Sincere thanks are due to AAGE BOHR for valuable theoretical discussions, to ALFRED HERMANSEN for coating the interferometer plates with multilayers, and to POUL STREANDER for the painstaking construction of the Fabry-Perot étalon. Furthermore, financial support from the *Carlsbergfond* and the *Statens almindelige Videnskabsfond* is gratefully acknowledged.

Physics Department,
University of Copenhagen

Isotope Laboratory, Physics Department
Royal Veterinary and Agricultural College,
Copenhagen

References

1) J. KOCH and E. RASMUSSEN: Phys. Rev. **76**, 1417 (1949).
2) J. C. Hubbs and G. M. GROSOF: Phys. Rev. **104**, 715 (1956).
3) J. T. LATOURETTE, W. E. QUINN and N. F. RAMSAY: Phys. Rev. **107**, 1202 (1957).
4) G. M. GROSOF, P. BUCK, W. LICHTEN, and I. I. RABI: Phys. Rev. Letters **1**, 214 (1958).
5) E. RASMUSSEN and V. MIDDELBOE: Mat. Fys. Medd. Dan. Vid. Selsk. **30**, no. 13 (1955).
6) E. RASMUSSEN (Dissertation): *De ædle Luftarters Spektrer*, 73 (1932).
7) A. BOHR, J. KOCH, and E. RASMUSSEN: Ark. f. Fys. **4**, 455 (1952).
8) H. B. G. CASIMIR: Teylers Tweede Genootschap, Haarlem (1936).

Indleveret til selskabet den 12. maj 1960.
Færdig fra trykkeriet den 5. september 1960.